Mechanistic Investigations on the Formation of Supramolecular Cylindrical Shaped Oligomers and Polymers by Living Ring Opening Metathesis Polymerization of a 7-Oxanorbornene Monomer Substituted with Two Tapered Monodendrons

V. Percec* and D. Schlueter

The W. M. Keck Laboratories for Organic Synthesis, Department of Macromolecular Science, Case Western Reserve University, Cleveland, Ohio 44106-7202

Received February 4, 1997; Revised Manuscript Received June 18, 1997[⊗]

ABSTRACT: The synthesis of the monomer *exo,exo*-5,6-bis[[[(3,4,5-tris((4-(dodecyl-1-oxy)benzyl)oxy)]-benzyl)oxy]carbonyl]-7-oxabicyclo[2.2.1]hept-2-ene (**4**), containing two tapered monodendrons and its living ring-opening metathesis polymerization initiated with $RuCl_2(=CHPh)(PCy_3)_2$ are discussed. Oligomers and polymers with narrow molecular weight distribution (M_w/M_n = 1.06−1.29) and degrees of polymerization (DP) from 6 to 120, which correspond to M_n from 12 600 to 252 800, were synthesized and characterized. The monomer (**4**) and the corresponding polymers (**5**) self-assemble into disklike and cylindrical shapes which produce an enantiotropic hexagonal columnar (Φ_h) liquid crystalline (LC) phase. The analysis of the Φ_h phase of the monomer, oligomers, and polymers as a function of the DP reveals four regions and mechanisms for the generation of the Φ_h phase, *i.e.*, below the DP which forms a disklike molecule, below the DP which corresponds to the maximum length of a disklike molecule (DP = 26), up to the DP which corresponds to the persistence length of the rodlike cylinder (DP = 64), and above this value.

Introduction

The synthesis and polymerization of monomers based on various monodendrons is investigated both in our laboratory[1] and other laboratories.[2−5] The structure of the monodendrons studied in our laboratory evolved from phasmidic and hemiphasmidic low molecular weight compounds[6] and their corresponding polymers.[7] Our dendritic monomers and their polymers[1] differ from those investigated in other laboratories[2−4] in that they produce supramolecular shapes which generate thermotropic nematic, smectic,[8] columar hexagonal (Φ_h),[1,7,9] and cubic[10] liquid crystalline (LC) phases. These LC phases allow the determination of the shape of the supramolecular and macromolecular dendrimers as well as of their monodendritic building blocks *via* X-ray diffraction experiments.[8,9,10] In the case of polymers which produce a cylindrical supramolecular shape which generates a Φ_h phase, the assembly of the polymer tapered side groups in a cylindrical shape induces a specific conformation to the polymer backbone which is not dependent on its tacticity.[1h] A more detailed mechanistic discussion of this concept is available in a brief review.[1f]

One of the most important tools required to elucidate the mechanism of supramolecular shape formation in oligomers and polymers obtained from dendritic building blocks is a suitable living polymerization technique. Previously we have been successful in the use of the cationic polymerization of monodendrons attached to vinyl ethers.[1a,7c] However, even though this polymerization tolerates a large variety of functional groups,[11] only polymers with low degrees of polymerization could be obtained.[1a,7c]

Recently, a new metathesis initiator, $RuCl_2(=CHPh)(PCy_3)_2$ was reported.[12,13] This air-stable initiator tolerates a wide variety of functional groups and solvents. The goal of this paper is to describe the synthesis of monomer **4**, which contains two tapered monodendritic groups, followed by its living ring opening metathesis polymerization. Both the monomer **4** and its oligomers and polymers with degrees of polymerization from 6 to 120 (*i.e.*, M_n = from 12 600 to 252 000) self-assemble into disklike and cylindrical supramolecular structures which form a thermotropic columnar hexagonal (Φ_h) LC phase. Characterization of the Φ_h phase by a variety of techniques provides for the first time access to the mechanism of formation of the supramolecular disklike and cylindrical shapes as a function of the DP, thus demonstrating the power of this polymerization technique for further studies.

Experimental Section

Materials. 1,3-Dicyclohexylcarbodiimide (DCC, 99%), $LiAlH_4$ (95%), 4-(dimethylamino)pyridine (DMAP, 99%), neutral chromatographic Al_2O_3 (all from Aldrich), chromatographic SiO_2 (Fisher), SiO_2 thin layer chromatography sheets with fluorescent indicator (Kodak), $RuCl_2(=CHPh)(PCy_3)_2$ (Strem Chemical Co.), and other conventional reagents were used as received. $RuCl_2(=CHPh)(PPh_3)_2$[12] was synthesized from $RuCl_2$-PPh_3 (Lancaster) and phenyldiazoalkane.[14] Furan (Aldrich, 99%) was washed twice with 5% KOH, dried over Na_2SO_4, filtered, and distilled from solid KOH under Ar. THF and Et_2O were dried over sodium/benzophenone ketyl and distilled under N_2. CH_2Cl_2 was distilled from CaH_2. 4-(Dimethylamino)-pyridinium p-toluenesulfonate (DPTS) was synthesized as previously described.[1e]

Techniques. ^1H and ^{13}C NMR (200 and 50 MHz respectively) spectra were recorded on a Varian Gemini 200 at 20 °C with a tetramethylsilane (TMS) internal standard. IR spectra were recorded on a Perkin-Elmer 1320 spectrometer. Relative molecular weights of polymers were measured by gel permeation chromatography (GPC) with a Perkin-Elmer Series 10 LC pump equipped with an LC-100 column oven (40 °C), a UV detector, and a Nelson 900 series integrator data station. A set of two Polymer Laboratories PL gel columns of 5×10^2 and 10^4 Å and THF eluent at 1 mL min^{-1} were used. Polystyrene standards were used for calibration. HPLC measurements were carried out with the same instrument. Melting points were obtained on a Thomas-Hoover capillary melting point apparatus and are uncorrected. Differential

[⊗] Abstract published in *Advance ACS Abstracts,* September 1, 1997.

S0024-9297(97)00157-5 CCC: $14.00

scanning calorimetry (DSC) measurements were recorded on a Perkin-Elmer DSC-7. Indium and zinc were used as calibration standards. Heating and cooling rates were 10 °C min^{-1}. First-order transitions are reported as the maximum of endothermic and minimum of exothermic peaks, and glass transitions are recorded as the middle of the change in heat capacity. An Olympus BX40 optical polarized microscope equipped with a Mettler FP82 hot stage and a Mettler FP80 central processor was used to observe thermal transitions and analyze anisotropic textures. Reflection X-ray diffraction patterns of oriented samples were recorded with a Rigaku 12 kW rotating-anode generator (Cu Kα) with a diffractometer. Densities were determined as described previously.[1g]

Monomer and Polymer Synthesis. Methyl 3,4,5-Tris[(4-(dodecyl-1-oxy)benzyl)oxy]benzoate (1). Methyl 3,4,5-tris[(4-(dodecyl-1-oxy)benzyl)oxy]benzoate (**1**) was synthesized according to a modified literature procedure.[15] From 54.7 g (0.176 mol) of *p*-(dodecyl-1-oxy)benzyl chloride and 10.20 g (0.055 mol) of methyl 3,4,5-trihydroxybenzoate were obtained 37.0 g (67%) of white crystals (acetone). ^{1}H NMR, δ ($CDCl_3$, TMS, ppm): 0.88 (t, 9H, C*H*$_3$, J = 6.6 Hz), 1.29 (overlapped m, 54H, $(CH_2)_9$), 1.78 (m, 6H, C*H*$_2$CH$_2$OPh), 3.88 (s, 3H, CO_2CH_3), 3.90−3.98 (overlapped t, 6H, C*H*$_2$OPh), 4.94 (s, 2H, PhC*H*$_2$OPh *para* to CO_2CH_3), 5.02 (s, 4H, PhC*H*$_2$OPh *meta* to CO_2CH_3), 6.65 (s, 2H, Ar*H ortho* to CO_2CH_3), 6.76 (d, 2H, Ar*H ortho* to CH_2O−, *para* to CO_2CH_3, J = 8.8 Hz), 6.88 (d, 4H, Ar*H ortho* to CH_2O−, *meta* to CO_2CH_3, J = 8.7 Hz), 7.26 (overlapped, 2H, Ar*H ortho* to −CH_2OPh, *para* to CO_2CH_3), 7.32 (d, 4H, Ar*H ortho* to −CH_2OPh, *meta* to CO_2CH_3, J = 8.7). ^{13}C NMR, δ ($CDCl_3$, TMS, ppm): 14.0 (*C*H$_3$), 22.6 (*C*H$_2$CH$_3$), 26.0−29.6 [(*C*H$_2$)$_8$], 31.9 (*C*H$_2$CH$_2$CH$_3$), 51.9 (CO_2*C*H$_3$), 67.9 (CH$_2$*C*H$_2$OAr), 71.0 (Ar*C*H$_2$OAr, *meta* to $-CO_2CH_3$), 74.6 (Ar*C*H$_2$OAr, *para* to $-CO_2CH_3$), 109.2 (Ar*C ortho* to $-CO_2CH_3$), 114.0−114.4 (Ar*C ortho* to $-OCH_2CH_2-$), 128.5−130.1 (Ar*C para* to $-CO_2CH_3$, Ar*C para* to $-OCH_2CH_2-$, Ar*C meta* to $-OCH_2CH_2-$), 142.5 (Ar*C ipso* to $-CO_2CH_3$), 152.6 (Ar*C meta* to $-CO_2CH_3$), 158.9 (Ar*C ipso* to $-OCH_2CH_2-$), 166.5 (*C*═O).

3,4,5-Tris[(4-(dodecyl-1-oxy)benzyl)oxy]benzyl Alcohol (2). 3,4,5-Tris[(4-(dodecyl-1-oxy)benzyl)oxy]benzyl alcohol (**2**) was synthesized using a modified literature procedure.[16] A 500 mL round bottom flask containing a Teflon coated magnetic stirring bar and equipped with a dropping funnel and N_2 inlet−outlet was flushed with N_2 and charged with 40 mL of THF and 0.485 g (12.8 mmol) of $LiAlH_4$. A solution of methyl 3,4,5-tris[(4-(dodecyl-1-oxy)benzyl)oxy]benzoate (**1**) (12.27 g, 12.16 mmol) in 150 mL of THF was added dropwise to the $LiAlH_4$/THF slurry over 1 h. The reaction mixture was stirred for 2 h further at which time ^{1}H NMR indicated complete reduction. The reaction was quenched by adding 0.5 mL of H_2O dropwise and then 0.5 mL of 15% NaOH and 1.5 mL of H_2O. The resulting precipitate was filtered, and the THF was evaporated off using a rotary evaporator. The crude product was recrystallized from hot acetone and yielded 11.05 g (93%) of a white crystalline solid. Thermal transitions and corresponding enthalpy changes are listed in Table 1 (lit.[2] DSC, k 76.5−80 Φ_h 81.5 i; with a second Φ_h phase below 50 °C on cooling). ^{1}H NMR, δ ($CDCl_3$, TMS, ppm): 0.88 (t, 9H, C*H*$_3$, J = 6.7 Hz), 1.29 (overlapped m, 54H, $(CH_2)_9$), 1.59 (s, 1H, CH$_2$O*H*), 1.78 (m, 6H, C*H*$_2$CH$_2$OPh), 3.89−3.98 (overlapped t, 6H, C*H*$_2$OPh), 4.56 (s, 2H, PhC*H*$_2$OH), 4.93 (s, 2H, PhC*H*$_2$OPh *para* to CH_2OH), 5.01 (s, 4H, PhC*H*$_2$OPh *meta* to CH_2OH), 6.65 (s, 2H, Ar*H ortho* to CH_2OH), 6.76 (d, 2H, Ar*H ortho* to CH_2O−, *para* to CH_2OH, J = 8.8 Hz), 6.88 (d, 4H, Ar*H ortho* to CH_2O−, *meta* to CH_2OH, J = 8.7 Hz), 7.26 (overlapped, 2H, Ar*H ortho* to −CH_2OPh, *para* to CH_2OH), 7.32 (d, 4H, Ar*H ortho* to −CH_2OPh, *meta* to CH_2OH, J = 8.7). ^{13}C NMR, δ ($CDCl_3$, TMS, ppm): 14.1 (*C*H$_3$), 22.6 (*C*H$_2$CH$_3$), 26.0−29.6 [(*C*H$_2$)$_8$], 31.9 (*C*H$_2$CH$_2$CH$_3$), 65.3 (Ar*C*H$_2$OH), 68.0 (*C*H$_2$OAr), 71.0 (Ar*C*H$_2$OAr, *meta* to CH_2OH), 74.8 (Ar*C*H$_2$OAr, *para* to CH_2OH), 106.6 (Ar*C ortho* to −CH_2OH), 114.1−114.4 (Ar*C ortho* to $-OCH_2CH_2-$), 129.1−130.2 (Ar*C para* to CH_2OH, Ar*C para* to $-OCH_2CH_2-$, Ar*C meta* to $-OCH_2CH_2-$), 136.5 (Ar*C ipso* to CH_2OH), 153.0 (Ar*C meta* to CH_2OH), 158.8 (Ar*C ipso* to $-OCH_2CH_2-$). IR, ν_{max}(cm^{-1}): 3200−3500 (OH). Purity (HPLC): 100%. TLC: R_f = 0.13 (3:1 hexanes/ethyl acetate).

***exo,exo*-5,6-Bis[[[(3,4,5-tris((4-(dodecyl-1-oxy)benzyl)-oxy)]benzyl)oxy]carbonyl]-7-oxabicyclo[2.2.1]hept-2-ene (4).** A 50 mL round bottom flask equipped with a Teflon-coated magnetic stirring bar was flushed with N_2 and charged with 1.51 g (1.53 mmol) of 3,4,5-tris[(4-(dodecyl-1-oxy)benzyl)-oxy]benzyl alcohol (**2**), 0.13 g (0.77 mmol) of **3**,[17] 0.015 g (0.12 mmol) of DMAP, and 8 mL of CH_2Cl_2. The reaction mixture was stirred for 48 h at 22 °C at which time ^{1}H NMR indicated complete alcoholysis of the anhydride. DCC (0.175 g, 0.847 mmol) and an additional portion of catalyst, DPTS (0.049 g, 0.154 mmol), were added to the reaction mixture. After 20 h, ^{1}H NMR indicated <1% of the starting alcohol remained. The reaction mixture was filtered and the solvent was removed by rotary evaporator. The crude product was chromatographed on SiO_2 using 3:1 hexanes/ethyl acetate and then precipitated into MeOH to yield 1.21 g (74%) of a white powder. Thermal transitions and corresponding enthalpy changes are listed in Table 1. ^{1}H NMR, δ ($CDCl_3$, TMS, ppm): 0.88 (t, 18H, C*H*$_3$, J = 6.9 Hz), 1.27 (overlapped m, 108H, $(CH_2)_9$), 1.78 (m, 12H, C*H*$_2$CH$_2$OPh), 2.84 (s, 2H, OCHC*H*CO_2), 3.86−3.95 (overlapped t, 12H, C*H*$_2$OPh), 4.76−4.95 (overlapped peaks, 16H, PhC*H*$_2$OPh, CO_2C*H*$_2$Ph), 5.25 (s, 2H, OC*H*CHCO$_2$), 6.46 (s, 2H, ═C*H*), 6.60 (s, 4H, Ar*H ortho* to $CH_2OC(O)$), 6.72 (d, 4H, Ar*H ortho* to CH_2CH_2O−, *para* to $CH_2OC(O)$, J = 8.5 Hz), 6.83 (d, 8H, Ar*H ortho* to CH_2O−, *meta* to $CH_2OC(O)$, J = 8.7 Hz), 7.20−7.29 (overlapped peaks, 12H, Ar*H ortho* to −CH_2OPh, *para* to $CH_2OC(O)$, and Ar*H ortho* to −CH_2OPh, *meta* to $CH_2OC(O)$). ^{13}C NMR, δ (C_6D_6, TMS, ppm): 14.4 (*C*H$_3$), 22.6 (*C*H$_2$CH$_3$), 26.0−30.2 [(*C*H$_2$)$_8$], 32.4 (*C*H$_2$CH$_2$CH$_3$), 47.7 (C(O)*C*H), 67.0 (Ar*C*H$_2$OC(O)), 67.9−68.0 (*C*H$_2$OAr), 71.3 (Ar*C*H$_2$OAr, *meta* to $-CH_2OC(O)$), 75.3 (Ar*C*H$_2$OAr, *para* to $-CH_2OC(O)$), 80.7 (C(O)CH*C*H(O)CH═), 108.2 (Ar*C ortho* to $-CH_2OC(O)$), 114.4−114.8 (Ar*C ortho* to $-OCH_2CH_2-$), 129.1−131.8 (Ar*C para* to $CH_2OC(O)$, Ar*C para* to $-OCH_2CH_2-$, Ar*C meta* to $-OCH_2CH_2-$), 136.8 (*C*H═*C*H), 139.3 (Ar*C ipso* to $CH_2OC(O)$), 153.8 (Ar*C meta* to $CH_2OC(O)$), 159.5 (Ar*C ipso* to $-OCH_2CH_2-$), 171.2 (*C*═O). Purity (HPLC): 100%. TLC: R_f = 0.49 (2:1 hexanes/ethyl acetate). Anal. Calcd for $C_{136}H_{200}O_{17}$: C, 77.52; H, 9.41. Found: C, 77.45; H, 9.33.

General Procedure for the Polymerization of 4 Initiated with $RuCl_2$(═CHPh)(PCy_3)$_2$ (5). The appropriate amount of monomer **4** (typically, 0.5−1.0 g) was placed in an oven-dried Schlenk tube containing a Teflon-coated magnetic stirring bar. The tube was sealed with a rubber septum and placed under vacuum, followed by an Ar backflush. Freshly distilled CH_2Cl_2 (enough to make a 50 wt % monomer solution) was transferred to the tube, and the solution was degassed by successive freeze−pump−thaw cycles. The proper amount of $RuCl_2$(═CHPh)(PCy_3)$_2$ (as indicated by the desired DP) was added to the stirred monomer solution. The tube was sealed and stirred, depending on the desired DP, from 3 to 24 h at 22 °C. The conversion was followed by sampling the reaction mixture followed by GPC analysis. The reaction was terminated by addition of about 2 mL of ethyl vinyl ether and stirring for at least 1 h. The polymer was purified by passing it through a basic Al_2O_3 column using hexanes eluent. Precipitation into MeOH resulted in a white polymer. Thermal transitions and corresponding enthalpy changes are listed in Table 1. ^{1}H NMR, δ ($CDCl_3$, TMS, ppm): 0.88 (t, 18H, C*H*$_3$, J = 6.9 Hz), 1.27 (overlapped peaks, 108H, $(CH_2)_9$), 1.78 (m, 12H, C*H*$_2$CH$_2$OPh), 3.00−3.20 (broad s, 2H, OCHC*H*CO_2), 3.61−3.82 (broad s, 12H, C*H*$_2$OPh), 4.45−4.82 (broad s, 18H, PhC*H*$_2$OPh, CO_2C*H*$_2$Ph; OC*H*CHCO$_2$), 5.80−5.95 (broad s, 2H, ═C*H*, *cis* and *trans*), 6.30−6.72 (overlapped peaks, 16H, Ar*H ortho* to $CH_2OC(O)$, 4H, Ar*H ortho* to CH_2CH_2O−, *para* to $CH_2OC(O)$), Ar*H ortho* to CH_2O−, *meta* to $CH_2OC(O)$), 6.89−7.19 (overlapped peaks, 12H, Ar*H ortho* to −CH_2OPh, *para* to $CH_2OC(O)$, and Ar*H ortho* to −CH_2OPh, *meta* to $CH_2OC(O)$). ^{13}C NMR, δ (C_6D_6, TMS, ppm): 14.8 (*C*H$_3$), 22.6 (*C*H$_2$CH$_3$), 27.2−30.2 [(*C*H$_2$)$_8$], 32.9 (*C*H$_2$CH$_2$CH$_3$), 54.0 (C(O)*C*H), 68.2−68.7 (Ar*C*H$_2$OC(O), *C*H$_2$OAr), 72.0 (Ar*C*H$_2$OAr, *meta* to $-CH_2OC(O)$), 75.8 (Ar*C*H$_2$OAr, *para* to $-CH_2OC(O)$), 78.6−79.2 (C(O)-CH*C*H(O)CH═, β to *cis*), 81.9−83.4 (C(O)CH*C*H(O)CH═, β to *trans*), 108.5 (Ar*C ortho* to $-CH_2OC(O)$), 114.9−115.3 (Ar*C ortho* to $-OCH_2CH_2-$), 129.1−130.8 (Ar*C para* to $CH_2OC(O)$, Ar*C para* to $-OCH_2CH_2-$, Ar*C meta* to $-OCH_2CH_2-$), 136.5−

Table 1. Characterization of 2, 4, and 5 by GPC and DSC Analysis with Data Collected from the First Heating and Cooling DSC Scans on the First Line, and Data from the Second Heating Scan on the Second Line (k = Crystalline Phase, Φ_h = Hexagonal Columnar Mesophase, i = Isotropic Phase)

compound	yield (%)[a]	DP[b]	$M_{n,GPC}$	$M_n/M_{n,GPC}$	M_w/M_n (GPC)	thermal transitions (°C) and enthalpy changes (kcal/mol or kcal/mru) heating	cooling
2	93					k 79, 82[c] (20.2) i	i 76 (0.62) Φ_h 47 (0.64) Φ_h' 31 (8.51) i
						k 46, 50[c] (5.34) k_1 55 (−12.7) k_2 75 (14.2) Φ_h 80 (0.61) i	
4	74					k 42, 57, 64[c] (23.3) Φ_h 71 (1.00) i	i 66 (1.06) Φ_h
						Φ_h 72 (1.06) i	
5	60	6	12 200	1.03	1.07	Φ_h 97 (0.89) i	i 88 (0.81) Φ_h
						Φ_h 97 (0.70) i	
5	65	9	13 200	1.40	1.08	Φ_h 97 (0.62) i	i 87 (0.73) Φ_h
						Φ_h 97 (0.63) i	
5	76	13	18 300	1.46	1.07	Φ_h 101 (0.60) i	i 90 (0.69) Φ_h
						Φ_h 102 (0.60) i	
5	64	14	16 500	1.82	1.09	Φ_h 102 (0.58) i	i 92 (0.66) Φ_h
						Φ_h 102 (0.61) i	
5	70	19	22 200	1.67	1.06	Φ_h 98 (0.65) i	i 82 (0.69) Φ_h
						Φ_h 99 (0.65) i	
5	51	25	26 800	1.96	1.08	Φ_h 103 (0.42) i	i 88 (0.66) Φ_h
						Φ_h 106 (0.36) i	
5	76	26	26 000	2.12	1.11	Φ_h 107 (0.70) i	i 90 (0.71) Φ_h
						Φ_h 107 (0.66) i	
5	76	29	27 800	2.19	1.12	Φ_h 114 (0.33) i	i 97 (0.41) Φ_h
						Φ_h 114 (0.40) i	
5	68	32	29 600	2.24	1.13	Φ_h 120 (0.26) i	i 102 (0.36) Φ_h
						Φ_h 120 (0.20) i	
5	68	33	38 100	1.82	1.12	Φ_h 122 (0.20) i	i 109 (0.33) Φ_h
						Φ_h 122 (0.19) i	
5	68	40	41 100	2.05	1.13	Φ_h 125 (0.23) i	i 112 (0.30) Φ_h
						Φ_h 125 (0.23) i	
5	78	49	44 800	2.29	1.10	Φ_h 130 (0.29) i	i 119 (0.29) Φ_h
						Φ_h 131 (0.22) i	
5	73	50	47 200	2.21	1.14	Φ_h 134 (0.32) i	i 122 (0.26) Φ_h
						Φ_h 134 (0.30) i	
5	79	57	58 100	2.06	1.23	Φ_h 142 (0.29) i	i 129 (0.28) Φ_h
						Φ_h 141 (0.27) i	
5	83	64	67 800	2.00	1.23	Φ_h 150 (0.20) i	i 134 (0.23) Φ_h
						Φ_h 149 (0.19) i	
5	80	77	65 700	2.44	1.25	Φ_h 145 (0.36) i	i 131 (0.33) Φ_h
						Φ_h 146 (0.33) i	
5	89	88	75 800	2.45	1.24	Φ_h 149 (0.26) i	i 133 (0.31) Φ_h
						Φ_h 148 (0.24) i	
5	80	102	82 300	2.60	1.26	Φ_h 148 (0.23) i	i 131 (0.30) Φ_h
						Φ_h 147 (0.22) i	
5	84	120	86 900	2.91	1.29	Φ_h 145 (0.35) i	i 128 (0.37) Φ_h
						Φ_h 144 (0.31) i	

[a] Isolated. [b] Corrected for conversion. [c] Combined enthalpy.

137.0 (*C*H=*C*H), 139.9 (Ar*C ipso* to $CH_2OC(O)$), 154.3 (Ar*C meta* to $CH_2OC(O)$), 160.0 (Ar*C ipso* to $-OCH_2CH_2-$), 171.5 (*C*=O).

Results and Discussion

Synthesis, Characterization, and Polymerization of Monomer 4. The synthesis of the 7-oxanorbornene monomer **4** was accomplished in two steps starting from the taper-shaped precursor methyl-3,4,5-tris[(4-(dodecyl-1-oxy)benzyl)oxy]benzoate (**1**)[15] (Scheme 1). The methyl ester was reduced with $LiAlH_4$ using a modified literature procedure.[16] Aqueous NaOH work-up produced the corresponding benzyl alcohol, 3,4,5-tris-[(4-(dodecyl-1-oxy)benzyl)oxy]benzyl alcohol (**2**) in 93% yield following recrystallization from acetone. The benzyl alcohol was subsequently esterified with the furan−maleic anhydride Diels−Alder adduct **3**.[17] The esterification proceeds in two steps in one pot *via* an ester−acid intermediate. Such a strategy would allow the ready placement of two dissimilar substituents on the same monomer unit, leading to the construction of a copolymer by the homopolymerization of a single monomer. In this case, however, the anhydride **3** was reacted with 2 equiv of **2** and a catalytic amount of the nucleophilic catalyst DMAP in CH_2Cl_2 for 48 h at 22 °C. Increased reaction temperatures lead to significant side products, presumably due to retro-Diels−Alder degradation of **3**. After 48 h ^{1}H NMR indicated consumption of 1 equiv of **2**. DCC and an additional portion of the nucleophilic catalyst DPTS were used to effect the esterification of the resulting acid with the remaining equivalent of **2**. Purification by column chromatography (SiO_2, 3:1 hexanes/ethyl acetate) afforded 74% yield of monomer **4**.

On the first DSC heating scan, monomer **4** displays a complex series of crystalline melting endotherms from 42 to 64 °C and transforms into an enantiotropic Φ_h phase which persists to 71 °C (Table 1). On cooling, the Φ_h phase re-forms at 66 °C, but the crystalline phase does not return, even on cooling to −20 °C. Subsequent heating scans show only the Φ_h to isotropic phase transition (72 °C). Optical polarized microscopy confirms the presence of a Φ_h phase as shown by the characteristic fan-shaped texture. The X-ray diffraction results obtained in the Φ_h phase of monomer **4** are summarized in Table 2 and confirm the assignment made by DSC and thermal optical polarized microscopy. The analysis of these X-ray results demonstrate that

Scheme 1. Synthesis of *exo,exo*-5,6-Bis[[[(3,4,5-tris((4-(dodecyl-1-oxy)benzyl)oxy)]benzyl)oxy]carbonyl]-7-oxabicyclo[2.2.1]hept-2-ene (4) and Its Polymerization to 5

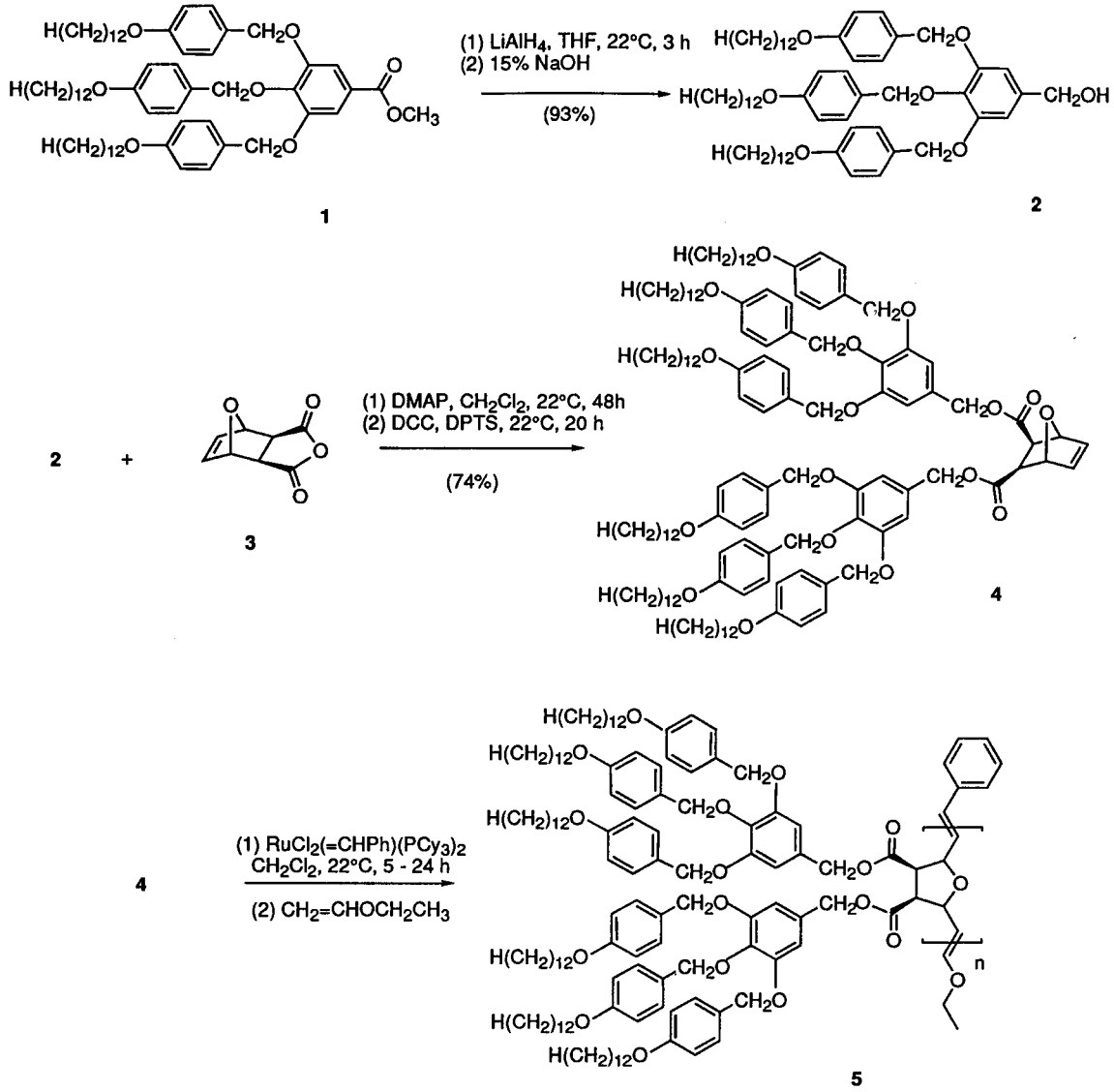

Table 2. Characterization of Monomer 4 and Polymer 5 by X-ray Diffraction Experiments

compound	temp (°C)	d_{100} (Å)	d_{110} (Å)	d_{200} (Å)	$\langle d_{100}\rangle$ (Å)[a]	a (Å)[b]	R (Å)[c]	S (Å)[d]	ρ[e]	μ[f]
4	60	37.44	(21.62)	19.38 (18.72)	38.10	43.99	22.00	25.40	1.05	1.88
5[g]	rt[h]	38.37	22.51 (22.15)	19.79 (19.19)	38.98	45.01	22.51	25.99	1.04	1.99

[a] $\langle d_{100}\rangle = (d_{100} + \sqrt{3}(d_{110}) + 2d_{200})/3$. [b] Column diameter, $a = 2\langle d_{100}\rangle/\sqrt{3}$. [c] Column radius, $R = \langle d_{100}\rangle/\sqrt{3}$. [d] Distance from column center to hexagon vertex, $S = 2R/\sqrt{3}$. [e] ρ = experimentally determined density at 20 °C (g/mL). [f] Number of repeat units in a cross section, $\mu = \rho(3\sqrt{3})N_A S^2 t/(2M)$ (for a detailed discussion of these calculations, see ref 20a). [g] $[M]_o/[I]_o = 28.9$. [h] Sample cooled from isotropic to roon temperature at −0.1 °C/min.

in the Φ_h phase two monomers **4** (*i.e.*, four tapered monodendritic groups) form the stratum of the column. Therefore, in the columnar structure **4** self-assembles in disklike supramolecular dimers.

The ring opening metathesis polymerization of **4** was performed by adding $RuCl_2(=CHPh)(PCy_3)_2$, to a degassed 50 wt % solution of **4** in CH_2Cl_2. Monomer **4** did not polymerize in the presence of the less active precursor, $RuCl_2(=CHPh)(PPh_3)_2$. The reaction time required to reach complete conversion depends on the target DP. The polymerization experiments directed to lower DPs required only a few hours to reach >95% conversion at 22 °C. The highest DPs required 24 h at 22 °C to reach high conversion. In all polymerizations conversions of higher than 95% were reached, and the reported DPs from Table 1 are corrected for conversion. The polymerization was terminated with an excess of ethyl vinyl ether and stirred for at least 1 h. The crude polymer was passed through a short column of basic Al_2O_3 (hexanes) to remove the Ru catalyst and the unreacted monomer and then was precipitated into methanol, filtered off, and dried under vacuum. This polymerization demonstrated a living character through the narrow polydispersity achieved and the linear dependence of $\ln([M]_o/[M])$ on time ($k_p = 2.03 \times 10^{-2}$ M^{-1} s^{-1}) (Figure 1). The polymer backbone microstruc-

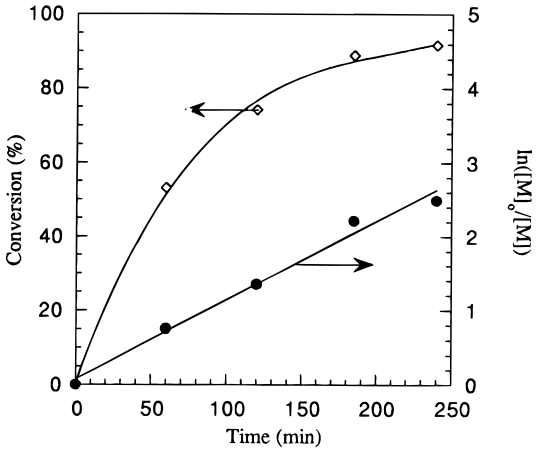

Figure 1. Plot of conversion vs time for the polymerization of **4** ($[M]_o/[I]_o = 50$).

ture was analyzed by inverse gated decoupled ^{13}C experiments.[1h] Integration of *cis*-CH=CH*C*HO (~78.8 ppm) vs *trans*-CH=CH*C*HO (~82.5 ppm) showed that the polymer backbone microstructure contained predominantly *trans* double bonds (24% *cis*, 76% *trans*) and was independent of the polymer DP.

Thermal and Structural Characterization of Polymer 5 (DP = 6−120). All oligomers and polymers **5** were characterized by a combination of techniques consisting of differential scanning calorimetry (DSC), X-ray scattering, and thermal optical polarized microscopy experiments. The transition temperatures and the associated enthalpy and entropy changes for each polymer synthesized were determined by DSC and are reported in Table 1. All oligomers and polymers display an enantiotropic Φ_h LC phase with a thermal stability that is determined by its DP.

The transition temperatures of **5** collected from heating and cooling DSC scans are plotted vs DP in Figure 2a. This plot can be divided in four different dependencies of $T_{\Phi h-i}$ and $T_{i-\Phi h}$ on DP, *i.e.*, from DP 1 to 6, from 6 to 26, from 26 to 64, and from 64 to 120. The first region (DP = 1−6) shows a 25 °C increase in the stability of the Φ_h LC phase on going from monomer **4** to the DP 6 oligomer. This represents the highest temperature increase per DP for the entire range of molecular weight (highest slope). The slope of this dependence decreases dramatically between DP 6 and DP 26, and increases again from DP 26 to DP 64. At higher DPs than 64 the isotropization temperature reaches a plateau.

The trend of $T_{\Phi h-i}$ vs DP from Figure 2a resembles a mirror-image of the dependence of $\Delta H_{i-\Phi h}$ and $\Delta S_{i-\Phi h}$ associated with the same transition temperatures on DP (Figure 2b). These two thermodynamic parameters are plotted as a function of DP in Figure 2b. Both $\Delta H_{i-\Phi h}$ and $\Delta S_{i-\Phi h}$ decrease sharply from DP 1 to DP 6. The slope of this dependence decreases from DP 6 to DP 26 and increases from DP 26 to DP 64. A plateau is reached at higher values of DP.

Before attempting to explain this dependence we should remember that in the case of both linear and hyperbranched main chain liquid crystalline polymers both the isotropization temperature and the corresponding enthalpic and entropic contributions associated with this transition follow the same trend; *i.e.*, they show a steep increase up to a certain DP, and after this value the slope of this dependence is smaller and can be

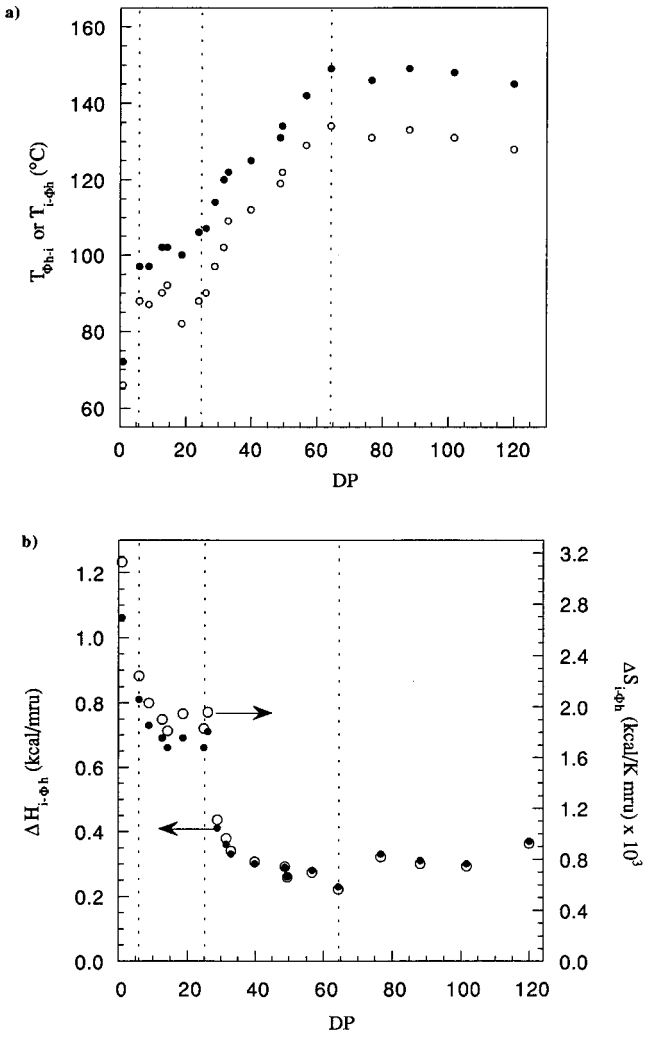

Figure 2. (a) Dependence of the phase transition temperatures, $T_{\Phi h-i}$ (l) and $T_{i-\Phi h}$ (○) on the degree of polymerization (DP) of **5**. (b) Dependence of the enthalpy (●) and entropy (○) changes on the degree of polymerization (DP) of **5**. DPs = 6, 26, and 64 are marked with dotted lines in both plots.

approximated with a plateau.[8,18] In the case of side chain liquid crystalline polymers the isotropization transition temperature follows the same trend as in the case of main chain liquid crystalline polymers, while the corresponding thermodynamic parameters appear to be independent of DP with the exception of very low DPs when they are influenced by the large contribution from the chain end.[19] This dependence is regarded as the *polymer effect*, which has been reviewed[20] and has also been the subject of various theoretical evaluations.[21]

A notable deviation from this behavior is provided by macrocyclic liquid crystals obtained from main chain type repeat units.[22] This class of molecules provides an odd−even dependence of their transition temperatures and thermodynamic parameters on DP. This odd−even dependence shows an increase followed by a maximum before it reaches a plateau. A second deviation from the conventional trend was observed in the case of a series of side chain liquid crystalline poly(vinyl ethers).[23] In this case, the isotropization temperatures follow the expected trend, however, their associated thermodynamic parameters show a small decrease with an increase in DP.[23] Therefore, the trends of both transition temperature and associated thermodynamic parameters on DP from Figure 2 do not have a precedent.

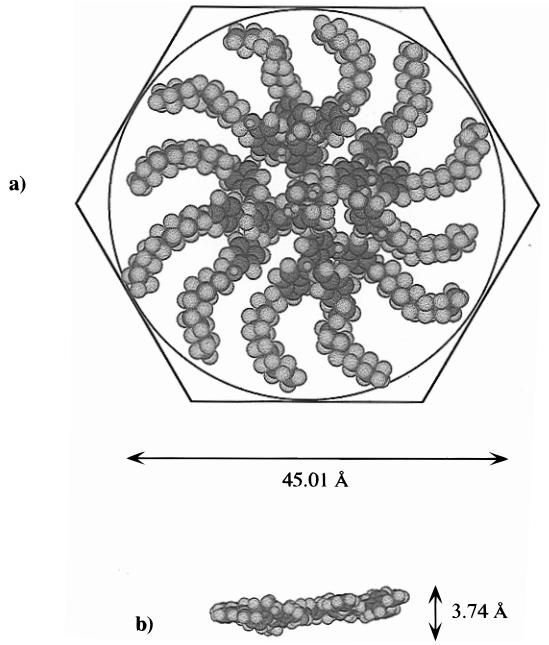

Figure 3. (a) Molecular model of a cross section of the supramolecular tubular architecture formed by **5** in the Φ_h phase. (b) Side view of part a (the alkyloxy tails have been omitted for clarity).

Let us first discuss the structure of polymer **5** in its Φ_h phase. The X-ray diffraction data from an unoriented sample of polymer **5** (DP = 28) is presented in Table 2. Diffractions in a ratio of $1:1/\sqrt{3}:1/\sqrt{4}$ which are characteristic of a Φ_h LC phase, are present at small angles with a diffuse scattering observed at wide angles. The texture formed by these polymers is typical of a Φ_h LC phase. Table 2 also summarizes the column radius (R, Å), the column diameter (a, Å), and the number of monomer units (μ) per column cross section or stratum (assuming a layer thickness of 3.74 Å).[24] From these results, an estimate of column length (L) at different DPs is possible and therefore we can discuss the dependencies from Figure 2a,b as a function of the molecular parameters of the cylindrical polymer **5**.

A molecular model of a cross section of polymer **5** in the Φ_h LC phase with a column diameter a (Å) is presented in Figure 3. As prescribed by the X-ray data, two monomer units, *i.e.*, four taper-shaped building blocks, occupy the column cross section. The model also suggests the presence of a polar central cavity lined with furanyl oxygens and carbonyl groups,[25] which is surrounded by a rigid aromatic shell and nonpolar aliphatic alkyl chains.[1h] This distribution of tapered groups contrasts with that previously reported for a related polymer containing the less bulky **12AG** taper-shaped substituents.[1h] In that case, the smaller size of the monomer required three repeat units to occupy a column layer. In the present case, the more sterically demanding dodecyloxy−benzyloxy substituents in polymer **5** fill the space sufficiently so that only two monomer units are required to fill one layer. This results in a more efficient packing of the taper-shaped units in the supramolecular column, as evidenced by the increased thermal stability of the resulting Φ_h LC phase, even at low DPs. Since $\mu = 1.99$, then two monomer units occupy 3.74 Å; therefore each monomer repeat unit adds 1.88 Å to the length (L) of the column. On the basis of this calculation, 24 monomer units are required for the length of the column to equal its diameter (45.01 Å). This length marks the transition from a disk-shaped molecule to a rod-shaped supermolecules. In the Φ_h phase, both the disk and the rod-shaped supermolecules self-assemble into a supramolecular cylindrical architecture (Scheme 2). Evidently these two mechanisms should produce columns of different rigidity and therefore, different dependencies of their $T_{\Phi h-i}$ and $T_{i-\Phi h}$ on DP are expected, and is indeed observed (Figure 2).

Therefore, the sharp increase in $T_{\Phi h-i}$ from DP 1 to DP 6 is due to the dramatic difference between the stability of a Φ_h LC phase generated from a supramolecular thin disk produced only *via* nonbonding interactions at DP 1 (disk length, L = 3.74 Å), and the disk produced by covalent bonding (DP 6, L = 11.3 Å). The change in slope of the dependence $T_{\Phi h-i}$ − DP (Figure 2a) from DP 6 to DP 26 is most probably due to the fact that the increase in the stability of the Φ_h LC phase is

Scheme 2. Schematic Representation of the Formation of Supramolecular Columns from Discrete Numbers of Tapered Monodendrons Where the Relationship between the Width and Height of the Supramolecular Columns Is Represented to Scale

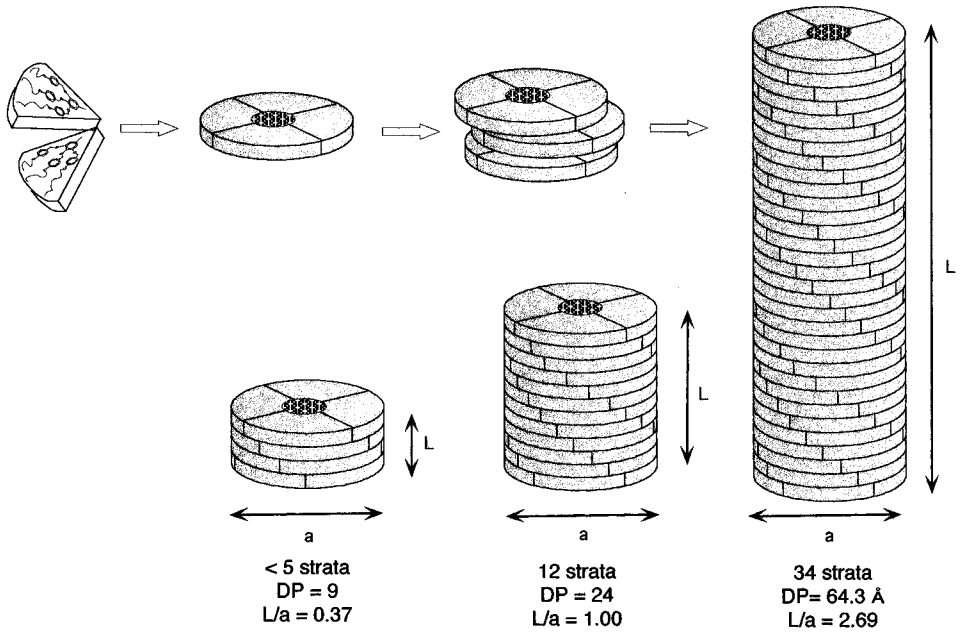

less affected by the change in covalent disk length than by the change in the mechanism of disk formation, *i.e.*, nonbonding vs covalent. Above DP 26 the shape of the polymer **5** becomes rodlike ($L/a > 1$). A continuous increase in the values of $T_{\Phi h-i}$ occurs up to DP 64. The length (L) of the cylinder of DP 64 is 120 Å. Above this value this dependence reaches a plateau. Recent results from our laboratory on the conformation of various polymer backbones jacketed with monodendrons have shown that their persistence length varies from 130 to 200 Å.[26] Therefore, it is reasonable to speculate that DP 64 may correspond to the persistence length of this polymer. Under these circumstances, between DP 26 and DP 64, polymer **5** is a three dimensional rodlike molecule, and therefore, $T_{\Phi h-i}$ should follow a linear dependence on DP. Above DP 64, the polymer becomes wormlike, and therefore, $T_{\Phi h-i}$ should be almost independent of DP, which is indeed the case (Figure 2a).

A possible explanation for the dependence of $\Delta H_{i-\Phi h}$ and $\Delta S_{i-\Phi h}$ on DP is as follows. When both $\Delta H_{i-\Phi h}$ and $\Delta S_{i-\Phi h}$ are decreasing, an increase in $T_{i-\Phi h}$ results only when the decrease in entropy is larger than the decrease in enthalpy ($T_{i-\Phi h} = \Delta H_{i-\Phi h}/\Delta S_{i-\Phi h}$). In this case, $\Delta H_{i-\Phi h}$ decreases by a factor of 4.6 while $\Delta S_{i-\Phi h}$ decreases by a factor of 5.5, between DP 1 and DP 64 (Figure 2b, Table 1).

The dependence of $\Delta H_{i-\Phi h}$ on DP from Figure 2b demonstrates that the highest order in the Φ_h phase is realized at DP 1, *i.e.*, when the column self-assembles from a supramolecular disk generated *via* nonbonding interactions. When DP increased, the $\Delta H_{i-\Phi h}$ decreases and follows a mirror-image trend with that associated with the $T_{i-\Phi h}$ dependence on DP. This dependence, although at first sight seeming unexpected, is in agreement with the mechanism advanced for the formation of these supramolecular cylindrical architectures from a polymer jacketed with a monodendritic coat. The self-assembly of the tapered monodendrons in a cylindrical shape induces a helical conformation to its polymer backbone. The penalty of this change in backbone conformation comes from the loss of the degree of order (entropic contribution) of the cylindrical shape generated by the tapered side groups. The restricted conformation generated by this mechanism and the restricted conformation of the melted alkyl tails which are packed into a constricted volume of the cylindrical geometry, produces an even higher decrease of the configurational entropy which is seen in the larger decrease of $\Delta S_{i-\Phi h}$ (Figure 2b). This represents information on the internal order of the helical structure and is apparently accounted for in the $\Delta S_{i-\Phi h}$ term. The overall result is the generation of a macromolecular Φ_h LC phase of lower order than the corresponding monomeric one, and one of higher rigidity imposed by conformational restrictions.

Characterization of Polymers 5 by GPC. The molecular weight and polydispersity of each polymer was determined by gel permeation chromatography (GPC) with reference to polystyrene standards (Table 1). The GPC molecular weight of the oligomeric species closely matches the theoretical DP as prescribed by the $[M]_o/[I]_o$ ratio with allowance for conversion. However, on increasing the molecular weight the GPC significantly underestimates the absolute molecular weight. Notably, polymers derived from monomers with smaller monodendron side groups match the PS standard molecular weight even at high degrees of polymerization.[27] This indicates a preference for altering the solution conformation of the polymer on going to higher DP. This trend indicates a contraction of the hydrodynamic volume occupied by a repeat unit as the polymer molecular weight increases, and this is in agreement with a very compact cylindrical polymer resulted from a chain conformation similar to that in the Φ_h phase.

Conclusions

Living polymerization of taper-shaped monodendrons was achieved using the well-defined ruthenium carbene initiator, $RuCl_2(=CHPh)(PCy_2)_3$. The polymerization proceeds to quantitative or nearly quantitative conversion in all cases. Molecular weight was controlled by manipulating the monomer to initiator ratio which permitted the formation of near monodisperse oligomers to narrow polydispersity high molecular weight polymers ($M_n > 250\,000$).

The polymerization of monomer **4** with $RuCl_2(=CHPh)(PCy_2)_3$ provided a means to studying the effect of molecular weight on the thermal properties and solution behavior of a supramolecular tubular architecture. The resulting polymers **5** all exhibit an enantiotropic Φ_h liquid crystalline phase. The DSC data indicate the existence of four regimes which are composed of discrete structural forms ranging from supramolecular assemblies of disklike molecules to three dimensional rigid cylindrical shapes and to wormlike polymers. The enthalpy and entropy changes associated with the $T_{i-\Phi h}$ support this hypothesis.

The GPC data provides information on the structural dimensions of **5** in solution relative to polystyrene standards. A deviation from the PS standard molecular weight occurs at relatively low molecular weight. The solution conformation of oligomers and polymers **5** is more compact than the corresponding PS standards, a trend which continues through to the high molecular weight polymers. This trend indicates a contraction of the hydrodynamic volume occupied by a repeat unit as the polymer molecular weight increases.

Acknowledgment. Financial support by the National Science Foundation (Grant DMR-9708581) is gratefully acknowledged. We are also grateful to Professor S. Z. D. Cheng of the University of Akron for the density and X-ray measurements.

References and Notes

(1) (a) Percec, V.; Lee, M.; Heck, J. A.; Blackwell, H.; Ungar, G., Alvarez-Castillo, A. *J. Mater. Chem.* **1992**, *2*, 1033. (b) Percec, V.; Heck, J.; Tomazos, D.; Falkenberg, F.; Blackwell, H.; Ungar, G. *J. Chem. Soc., Perkin Trans. 1* **1993**, 2799. (c) Percec, V.; Heck, J. A.; Tomazos, D.; Ungar, G. *J. Chem. Soc., Perkin Trans. 2* **1993**, 2381. (d) Percec, V.; Heck, J.; Johansson, G.; Tomazos, D. *Macromol. Symp.* **1994**, *77*, 237. (e) Percec, V.; Schlueter, D.; Kwon, Y.-K.; Blackwell, J.; Möller, M.; Slangen, P. J. *Macromolecules* **1995**, *28*, 8807. (f) Percec, V.; Johansson, G.; Schlueter, D.; Ronda, J. C.; Ungar, G. *Macromol. Symp.* **1996**, *101*, 43. (g) Percec, V.; Johansson, G.; Ungar, G.; Zhao, J. P. *Macromolecules* **1996**, *29*, 646. (h) Percec, V.; Schlueter, D.; Ronda, J. C.; Johansson, G.; Ungar, G.; Zhou, J. P. *Macromolecules* **1996**, *29*, 1464. (i) Kwon, Y.-K.; Chvalun, S.; Schneider, A.-I.; Blackwell, J.; Percec, V.; Heck, J. A. *Macromolecules* **1994**, *27*, 6129. (j) Kwon, Y.-K.; Danko, C.; Chvalun, S.; Blackwell, J.; Percec, V.; Heck, J. A. *Macromol. Symp.* **1994**, *87*, 103. (k) Kwon, Y.-K.; Chvalun, S.; Blackwell, J.; Percec, V.; Heck, J. A. *Macromolecules* **1995**, *28*, 1552.

(2) (a) Hawker, C. J.; Fréchet, J. M. J. *Polymer* **1992**, *33*, 1507. (b) Fréchet, J. M. J.; Gitsov, I. *Macromol. Symp.* **1995**, *98*, 441.

(3) (a) Neubert, I.; Klopsch, R.; Claussen, W.; Schlüter, A.-D. *Acta Polym.* **1996**, *4A*, 455; (b) Neubert, I.; Kirstein, E. A.; Schlüter, A.-D., Dautzenberg, H. *Macromol. Rapid Commun.* **1996**, *17*, 517.
(4) Draheim, G.; Ritter, H. *Macromol. Chem. Phys.* **1995**, *196*, 2211.
(5) Chen, Y.-M.; Chen, C.-F.; Liu, W.-H.; Li, F.-Y.; Xi, F. *Macromol. Rapid Commun.* **1996**, *17*, 401.
(6) For a recent review on phasmidic molecules, see: Malthête, J.; Nguyen, T.; Destrade, C. *Liq. Cryst.* **1993**, *13*, 171.
(7) (a) Percec, V.; Heck, J. *J. Polym. Sci.: Part A: Polym. Chem.* **1991**, *29*, 591. (b) Percec, V.; Heck, J.; Ungar, G. *Macromolecules* **1991**, *24*, 4957; (c) Percec, V.; Lee, M.; Heck, J.; Blackwell, H. E.; Ungar, G.; Alvarez-Castillo, A. *J. Mater. Chem.* **1992**, *2*, 931.
(8) Percec, V.; Chu, P.; Ungar, G.; Zhou, J. *J. Am. Chem. Soc.* **1995**, *117*, 11441.
(9) Percec, V.; Johansson, G.; Ungar, G.; Zhou, J. *J. Am. Chem. Soc.* **1996**, *118*, 9855.
(10) Balagurusamy, V. S. K.; Ungar, G.; Percec, V.; Johansson, G. *J. Am. Chem. Soc.* **1997**, *119*, 1539.
(11) For a brief review on the polymerization of functional vinyl ethers by living cationic polymerization, see: Percec, V.; Tomazos, D. *Adv. Mater.* **1992**, *4*, 548.
(12) Grubbs, R. H.; Schwab, P.; France, M. B.; Ziller, J. W. *Angew. Chem., Int. Ed. Engl.* **1995**, *34*, 2039.
(13) (a) Grubbs, R. H.; Lynn, D. M.; Kanaoka, S. *J. Am. Chem. Soc.* **1996**, *118*, 784. (b) Grubbs, R. H.; Weck, M.; Schwab, P. *Macromolecules* **1996**, *29*, 1789. (c) Grubbs, R. H.; Weck, M.; Maughon, B. R.; Mohr, B. *Polym. Prepr. (Am. Chem. Soc., Div. Polym. Chem.)* **1996**, *37* (1), 587.
(14) Creary, X. *Org. Synth., Collect. Vol. VII*, 438.
(15) (a) Malthête, J.; Tinh, N. H.; Levelut, A. M. *J. Chem. Soc., Chem. Commun.* **1986**, 1548; (b) Percec, V.; Heck, J. *J. Polym. Sci., Part A: Polym. Chem.* **1991**, *29*, 591.
(16) Malthête, J.; Davidson, P. *Bull. Soc. Chim. Fr.* **1994**, *131*, 812.
(17) Diels, O.; Alder, K. *Chem. Ber.* **1929**, *62*, 557.
(18) Percec, V.; Kawasumi, M. *Macromolecules* **1993**, *26*, 1993.
(19) (a) Percec, V.; Tomazos, D.; Pugh, C. *Macromolecules* **1989**, *22*, 3259. (b) Percec, V.; Hahn, B. *Macromolecules* **1989**, *22*, 1588.
(20) (a) Percec, V.; Tomazos, D. in *Comprehensive Polymer Science*, Allen, G., Ed., Permagon Press, Oxford, England, 1992; First Suppl. pp 299−384. (b) Percec, V.; Pugh, C. In *Side Chain Liquid Crystal Polymers*; McArdle, C. B., Ed.; Blackie and Son Ltd., Chapman and Hall: Glasgow and New York, 1989; pp 30−105. (c) Pugh, C.; Kiste, A. L. *Prog. Polym. Sci.*, in press; (d) Percec, V. In *Handbook of Liquid Crystal Research*; Collings, P. G., Patel, J. S., Eds., Oxford University Press: Oxford, England, 1996; pp 259−346.
(21) (a) Percec, V.; Keller, A. *Macromolecules* **1990**, *23*, 4347. (b) Stevens, H.; Rehage, G.; Finkelmann, H. *Macromolecules* **1984**, *17*, 851.
(22) (a) Percec, V. *Pure Appl. Chem.* **1995**, *67*, 2031. (b) For a recent publication, see: Percec, V.; Turkaly, P. J.; Asandei, A. D. *Macromolecules* **1997**, *30*, 943.
(23) Gedde, U. W.; Jonsson, H.; Hult, A.; Percec, V. *Polymer* **1992**, *33*, 4352.
(24) (a) Percec, V.; Johansson, G.; Heck, J.; Ungar, G.; Batty, S. V. *J. Chem. Soc., Perkin Trans. 1* **1993**, 1411. (b) Safinua, C. R.; Liang, K. S.; Varady, W. A.; Clark, N. A.; Anderson, G. *Phys. Rev. Lett.* **1983**, *53*, 1172.
(25) (a) Novak, B. M.; Grubbs, R. H. *J. Am. Chem. Soc.* **1988**, *110*, 960. (b) Novak, B. M.; Grubbs, R. H. *J. Am. Chem. Soc.* **1988**, *110*, 7542.
(26) Percec, V.; Schlueter, D.; Ahn, C.-H.; Jamieson, A.; Schmidt, M. Unpublished results.
(27) Percec, V.; Schlueter, D. Unpublished results.

MA970157K